A Vectorcardiographic Approach to Understanding the 12-Lead Electrocardiogram of Atrial Flutter

J Ng, AV Sahakian, WG Fisher, S Swiryn

Northwestern University, Evanston, IL, USA

Abstract

We hypothesized that phase relationships of atrial flutter waves among different ECG leads could be used to discriminate atrial flutter mechanisms and that vectorcardiography could be used to identify such phase relationships.

Twenty-seven ECGs reflecting counterclockwise (CCW) isthmus-dependent (ID) flutter and eight ECGs reflecting clockwise (CW) ID flutter were reviewed. Vector analysis identified the following chronologic sequence in the ECGs of 24 of the 27 CCW ID flutter vector loops: iso-electric in all leads, trough in II, peak in V1, peak in II, and trough in V1. The CW ID flutter ECGs had the reverse sequence in II and V1.

The phase relationships of Leads II and V1 track the CCW and CW activation sequences of ID flutter, even for ECGs not satisfying the prevalent polarity and morphology criteria.

1. Introduction

The ECG criteria for typical atrial flutter are negative sawtooth waves in the inferior leads and upright waves in Lead V1. Variability of flutter wave morphology from patient to patient can make it difficult to differentiate typical flutter from atypical forms.

The activation sequence for typical flutter reflects a macroreentrant circuit in the right atrium bounded anteriorly by the tricuspid annulus [1]. The circuit around the annulus is counterclockwise when viewed from a left anterior oblique perspective while the left atrium is passively activated. An important characteristic of this particular mechanism of atrial flutter is the dependency of the circuit on a narrow isthmus in the lower right atrium between the tricuspid valve and the inferior vena cava [2]. Typical flutter is therefore also commonly known as isthmus-dependent atrial flutter. Typical flutter is now regularly treated by radio-frequency ablation of the isthmus, which has been shown to terminate the flutter and prevent recurrence [3,4].

A clockwise and less frequently occurring counterpart of typical flutter also exists, which can similarly be treated with ablation of the isthmus. The ECG criteria commonly used to identify clockwise isthmus-dependent flutter are upright waves in the inferior leads. However, similar waveforms can occur in non-isthmus dependent mechanisms of atrial flutter.

We have previously demonstrated that both clockwise and counterclockwise isthmus-dependent flutter have vector loop characteristics that suggest that the flutter waves strongly reflect the macroreentrant circuit in the right atrium [5,6]. The orientation of the vector loops were shown to be generally parallel to the tricuspid valve and the magnitude of the vectors corresponded in timing to the activation of areas where increased and decreased conduction velocity are known to exist. This observation was in contrast to previous reports in a dog model that the polarity of flutter waves was dependent on left atrial activation [7].

Despite the known utility of vectorcardiography to identify differences in conduction patterns, such displays currently are rarely used in the clinical setting. Because of this, the aim for this study was to obtain a better understanding of how isthmus-dependent flutter is reflected in the 12-lead ECG using vector loops and known activation points as references for this analysis. It was hypothesized that the elliptical morphology of the vector loops requires deterministic phase offsets between different leads and that these phase relationships offer additional criteria that could be used to better distinguish flutter mechanisms.

2. Methods

Twelve-lead ECGs during isthmus-dependent atrial flutter from patients undergoing ablation were retrieved from the physiologic recorder (Prucka Cardiolab/GE Medical Systems, Milwaukee, WI). Simultaneous bipolar intra-cardiac recordings from decapolar catheters placed along the lateral right atrial and coronary sinus were also retrieved. The tricuspid valve-inferior vena cava isthmus dependency was determined by entrainment criteria and termination of the flutter following ablation of the isthmus. The activation direction around the tricuspid valve was determined by mapping of the lateral right atrium and coronary sinus. Only ECGs in which an entire

0276–6547/04 $20.00 © 2004 IEEE

Computers in Cardiology 2004;31:629–632.

cycle of a flutter wave could be extracted without being obscured by QRS complexes and T waves were included in this study (e.g. flutter ECGs with 2:1 atrial-to-ventricular conduction ratios were excluded). Retrieval of these ECGs was approved by the Institutional Review Board of Evanston Hospital.

Due to the generally low amplitude of the atrial signals, multiple flutter cycles from each ECG were signal averaged to improve the signal-to-noise ratio. The maximum negative slopes of the bipolar electrograms from the lateral right atrium were used as the fiducial point of the flutter cycle. Morphology and polarity of the ECG flutter waves from leads II, V1 and V6 were analyzed and categorized as being primarily positive (POS), primarily negative (NEG), biphasic (BI), or iso-electric (ISO) with the mean amplitude of the signal chosen as iso-electric line.

Vector loops were derived from the 12-lead flutter ECGs by first downsampling the signals from the original 977 Hz sample rate to 97.7 Hz and then applying the inverse Dower transformation to obtain an orthogonal Frank-lead ECG [8]. We have previously demonstrated that viewing isthmus-dependent atrial flutter vector loops from the left anterior oblique view, much of the information of the activation sequence of the flutter could be ascertained [5,6], thus the vector loops were analyzed from this view in this study.

Specific points of the ECGs and instantaneous vectors of the vectorcardigram were compared with the activation times obtained from the bipolar intracardiac recordings. Flutter wave morphologies were compared using the activation time of the proximal coronary sinus as the reference and the general phase relationships defined by the timing comparisons of peaks and troughs between leads were determined.

3. Results

3.1. Patients

Thirty-five surface ECGs from 34 patients (26 male /8 female, mean age of 67 ± 10 yrs) were reviewed. Twenty-seven ECGs reflected counterclockwise flutter and eight ECGs reflected clockwise flutter. One patient had counterclockwise flutter at the start of the procedure that spontaneously terminated and later had induced clockwise flutter.

3.2. ECG characteristics

The 27 counterclockwise flutter ECGs had cycle lengths ranging from 207 ms to 303 ms (mean 243 ± 25 ms), while the eight clockwise flutter ECGs had cycle lengths ranging from 203 ms to 303 ms (mean 250 ± 30 ms). There was therefore no ability to differentiate flutter mechanisms based on cycle length.

Table 1 summarizes the flutter wave morphologies of the counterclockwise atial flutter ECGs. For the flutter waves that were biphasic, the order of the positive and negative deflections was also noted. For example, in Lead II of 24 of the 27 ECGs during counterclockwise flutter, the time of proximal coronary sinus activation was followed by a negative deflection then a positive deflection of nearly equal amplitude. The prevalent combination of morphology for counterclockwise flutter was biphasic in Lead II, positive in Lead V1, and negative in Lead V6.

Table 1. Counterclockwise flutter wave morphology

Lead	POS	NEG	BI	ISO
II	1	2	24 (-/+)	0
V1	25	0	1 (+/-)	1
V6	0	17	9 (-/+)	1

Table 2 summarizes the flutter wave morphologies for eight clockwise flutter ECGs. More variability was seen in the clockwise flutter ECGs when compared with the counterclockwise ECGs.

Table 2. Clockwise flutter wave morphology

Lead	POS	NEG	BI	ISO
II	3	2	3 (-/+)	0
V1	3	2	2 (-/+) 1 (+/-)	0
V6	4	2	1 (-/+)	1

The typical ECG morphologies of A) counterclockwise flutter and B) clockwise flutter are shown in Figure 1. Two consecutive cycles of each type are shown with the time of proximal coronary sinus activation marking the start of each tracing. The scale is 0.1 mV per mm and 40 ms per mm.

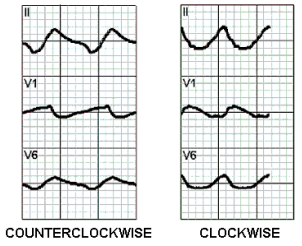

Figure 1. Prevalent ECG morphologies of A) counterclockwise flutter and B) clockwise flutter.

3.3. Vector characteristics

Twenty-four of the 27 vector loops of clockwise flutter

had clear counterclockwise rotations when viewed from the left anterior oblique view. The remaining three loops were narrow with no clear rotation direction and had low amplitude in Lead V1. The vector loops were elliptical in shape with a faster downward progression and slower upward progression. All of the eight vector loops of clockwise flutter had clear clockwise rotations in the left anterior oblique view but had more variation in morphology than counterclockwise flutter.

Examples of typical vector loop morphologies corresponding to the flutter waves in Figure 1 are shown in Figure 2. The time of proximal coronary sinus (Prox CS) activation is noted for each vector loop.

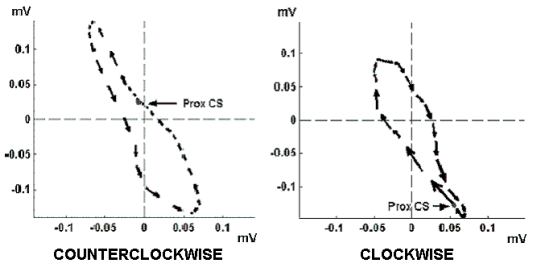

Figure 2. Prevalent vector loop morphologies of counterclockwise flutter and clockwise flutter corresponding to the ECGs of Figure 1.

3.4. ECG and vector correlations with intra-cardiac recordings

For all 27 counterclockwise flutter patients, activation at the proximal coronary sinus occurred during or near the time of upward vector progression where the arrows were the most crowded, as illustrated in Figure 2A. This time period of crowding of the arrows is synchronous to the most iso-electric (smallest sloped) regions of the ECG flutter wave.

As the coronary sinus is activated distally, the vectors are rotated counterclockwise around the upper portion of the loop. Lead II is at its trough at this time. This is followed by inferior activation of the lateral right atrium, which corresponds to the counterclockwise rotation of the vectors along the lower portion of the loop. In the ECG, the peak of Lead V1 occurs during the activation of the high lateral right atrium while the peak of Lead II occurs during low lateral right atrium activation.

In summary, the flutter wave sequence in the ECG starting from proximal coronary sinus activation is: iso-electric in all leads, trough in Lead II, peak in Lead V1, peak in Lead II, and trough in Lead V1.

For the clockwise flutter cases, proximal coronary sinus activation was not consistently near the regions of crowding of vector loop arrows. However, it did correspond consistently to the lower portion of the vector loop and the peak of Lead II. The distal activation of the coronary sinus corresponded to clockwise rotation following the lower left of the loop and the peak of Lead V1. The superior activation of the lateral right atrium corresponded to rotation of vectors along the top of the loop and the trough of Lead II.

As expected, the flutter wave sequence of clockwise flutter was reverse of the sequence of counterclockwise flutter: peak in Lead II, peak in Lead V1, trough in Leak II, and trough in Lead V1.

3.5. Vector loops derived from Leads II and V1

The sequences of peaks and troughs in Leads II and V1 were consistent for all but one counterclockwise flutter case. Therefore, vector diagrams using only Lead II against Lead V1 were generated. As expected, there were clear counterclockwise loops for 26 of 27 counterclockwise flutter cases and clear clockwise loops for all eight clockwise flutter cases. The loops generally were less elliptical and more circular using this method. Figure 3 show the II/V1 vector loop of the same ECG as Figures 1 and 2.

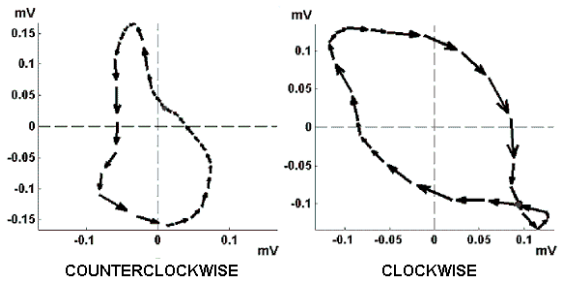

Figure 3. Vector loops generated using Leads II and V1 for counterclockwise and clockwise flutter.

3.6. Analysis of ECGs with atypical morphology

It can be seen from Tables 1 and 2 that there are likely flutter wave morphologies common to both mechanisms. However, the above results show that either vector loop analysis or ECG phase analysis can be used to discriminate between the two.

An example of such a situation is shown in Figure 4. The II/V1 vector loop and ECG on the top panel is a counterclockwise case despite seemingly upright waves in Lead II when one would expect biphasic or negative waves. The bottom panel is the vector loop and ECG of clockwise flutter with a similar ECG morphology. The difference in vector loop rotation direction can be readily

seen. However, with close inspection the typical differences in the sequence of troughs and peaks can also be seen.

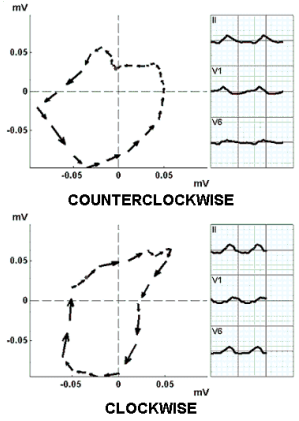

Figure 4. Vector loops and ECGs of A) counterclockwise and B) clockwise flutter with similar ECG morphologies.

4. Discussion

Using traditional ECG morphology and polarity criteria, a large percentage of typical atrial flutters can be identified as common practice has shown. However, we have found multiple cases in this study where counterclockwise isthmus-dependent flutter could not have been identified as such using morphology criteria. They potentially could have been deemed an atypical case thus making them a less ideal candidate for isthmus ablation.

The finding that vector loops are highly reflective of the activation sequence in the right atrium opens the possibility that additional information could be obtained by paying attention to the phase relationships of different leads. Warner et al. took advantage of similar ECG/VCG relationships to propose improved criteria for diagnosis of combined inferior myocardial infarction and left anterior hemiblock from scalar QRS complexes [9]. For the analysis of atrial flutter, an inferior lead and Lead V1 probably best approximate the coordinate axes in the left anterior oblique view of the vectorcardiogram. A positive amplitude in an inferior lead would correspond to a vector component pointing in the negative Y direction while a positive amplitude in Lead V1 would correspond to a vector component in the negative X direction. The construction of vector loops using only the two standard leads appeared to improve the ability to distinguish mechanisms when compared to using the derived orthogonal signals.

5. Conclusions

The phase relationships of Leads II and V1, whose directions approximate the coordinate axes of the LAO view, track the CCW and CW activation sequences of isthmus-dependent flutter. Vector loops and phase analysis of the ECG could differentiate flutter mechanisms having similar morphologies and polarities in the surface ECG.

Acknowledgements

The authors would like to thank Simona Petrutiu for her contributions to this paper.

References

[1] Cosio FG, Arribas F, Lopez-Gil M, et al. Catheter Mapping Studies in Atrial Flutter. In: Waldo AL, Touboul P. Atrial Flutter: Advances in Mechanisms and Management 1996. Armonk, NY: Futura Publishing Company, Inc. 1996:269-83.

[2] Feld GK, Fleck RP, Chen PS, et al. Radiofrequency catheter ablation for the treatment of human Type 1 atrial flutter: identification of a critical zone in the reentrant circuit by endocardial mapping techniques. Circulation 1992;86:1233-40.

[3] Cosio FG, Lopezgil M, Goicolea A, Arribas F, Barroso JL. Radiofrequency abation of the inferior vena cava-tricuspid valve isthmus in common atrial flutter. Am J Cardiol 1993;71:705-9.

[4] Lesh MD, Van Hare GF, Epstein LM, et al. Radiofrequency catheter ablation of atrial arrhythmias: results and mechanisms. Circulation 1994;89:1074-89.

[5] Ng J, Sahakian AV, Fisher WG, Swiryn S. Atrial flutter loops derived from the surface ECG: does the plane of the loop correspond anatomically to the macro-reentrant circuit?. J Electrocardiol 2003; 36(Suppl):181-6.

[6] Ng J, Sahakian AV, Fisher WG, Swiryn S. Discrimination of atrial flutter mechanisms from vector analysis of surface electrocardiograms. Pacing Clin Electrophysiol 2003; 26(abst.): 991.

[7] Olshansky B, Okumura K, Hess PG, et al. Demonstration of an area of slow conduction in human atrial flutter. J Am Coll Cardiol 1990;16:1639-48.

[8] Edenbrandt L, Pahlm O. Vectorcardiogram synthesized from a 12-lead ECG: Superiority of the inverse Dower matrix. J Electrocardiol. 1988; 21:361-7.

[9] Warner RA, Hill NE, Mookherjee S, Smulyan H. Electrocardiographic criteria for the diagnosis of combined inferior myocardial infarction and left anterior hemiblock. Am J Cardiol 1983;51:718-22.

Address for correspondence

Alan V. Sahakian, Ph.D.
2145 Sheridan Road
Evanston, IL 60208, USA
sahakian@ece.northwestern.edu